Apoptosis 2005; **10**: 909–920

Caspase-independent apoptosis is activated by diazepam-induced mitotic failure in HeLa cells, but not in human primary fibroblasts

I. Vitale, A. Antoccia, P. Crateri, S. Leone, G. Arancia and C. Tanzarella

Department of Biology, University "Roma Tre" , V.le Marconi 446, 00146 Rome, Italy (I. Vitale, A. Antoccia, S. Leone, C. Tanzarella); Department of Technology and Health, Istituto Superiore di Sanità, Viale Regina Elena 299, 00161 Rome, Italy (P. Crateri, G. Arancia)

DZ, a benzodiazepine known to affect centrosome separation at prophase, leads to a higher degree of mitotic arrest in HeLa cells than in primary human fibroblasts. In fact, differently from fibroblasts, which undergo a transient block in prophase-to-prometaphase transition, a high proportion of tumor cells attempt to escape from the DZ-imposed mitotic block, fail to undergo complete mitosis and die by mitotic failure. DZ-treated samples showed certain biochemical hallmarks of apoptosis, such as induction of the proapototic Bax protein, mitochondrial alterations assessed by JC-1 staining and TEM analysis, PARP cleavage, and DNA fragmentation. However, in DZ-treated cells, we observed a very low or absent caspase activation as shown by immunofluorescence and immunoblot experiments with antibodies directed to activated caspases and by staining with the pan-caspase inhibitor FITC-VAD-FMK. Experiments on mitochondrial depolymerization and apoptosis induction carried out in the presence of specific inhibitors of caspase-2 and caspase-3/7 indicated a caspase-independent apoptotic process induced by DZ. Accordingly, TEM analysis of treated cells revealed ultrastructural features resembling those reported for caspase-independent apoptosis. In conclusion, we hypothesize that HeLa cells override the prophase block imposed by DZ, producing a high rate of aberrant pro-metaphases, which, in turn, activates caspase-independent, apoptosis-like mitotic catastrophe.

Keywords: caspase-3; caspase-9; cell death; centrosome; diazepam; mitotic catastrophe.

Introduction

Programmed cell death is an essential process in development. In addition to this, apoptosis can be induced both in *in vitro* and *in vivo* systems by a variety of toxic stimuli, including DNA damage and ligand activated molecules.[1–3]

Morphological criteria such as chromatin condensation, collapse into highly condensed bodies, and internucleosomal DNA fragmentation, define apoptosis. Typical morphological alterations are also accompanied by specific biochemical changes, among which MMP (mitochondrial membrane permeability), phosphatidyl exposure and activation of caspases[4] are the more relevant.

An imbalance between pro- and anti-apoptotic Bcl-2 family members may lead to the release from the mitochondrion of factors such as cytochrome c, Apaf-1, AIF (apoptosis-inducing factor), and Smac/Diablo (second mitochondria-derived activator of caspase), which are in turn responsible for the activation of initiator factors and execution caspases.[4,5]

Microtubule-interfering agents are able to induce mitotic arrest and apoptosis by disruption or stabilization of the mitotic spindle in dividing cells.[6] Furthermore, functioning spindle poles have been reported to protect cells from apoptosis. In fact, the overduplication or failed separation of centrosomes leading to multipolar mitosis and failure in chromosome segregation, respectively, trigger cell death,[7,8] although the molecular pathways is yet to be elucidated.

The failure to complete mitosis in the presence of disturbing agents has also been termed "mitotic catastrophe", a type of cell death resulting from a combination of deficient cell-cycle checkpoints and cellular damage.[9] In this condition cells are prevented from arresting before or at mitosis, and show chromosomal aberrant segregation, which is responsible for the activation of an apoptotic pathway, usually ending with the formation of multinucleated cells displaying decondensed chromatin.[10,11]

Many different molecules are involved in mitotic failure or mitotic catastrophe. Among them, an aberrant mitotic entry, before completion of DNA synthesis, has been attributed to a premature nuclear entry and activation of the Cdk1(cyclin-dependent kinase 1)/cyclinB1 complex, or to inhibition of the checkpoint kinase Chk2.[9] Following induction of DNA damage, Chk2 colocalizes and interacts with Plk1 (Polo-like kinase) at centrosomes,[12] and is responsible for the phosphorylation of several key

Correspondence to: Antonio Antoccia, University "Roma Tre", V.le Marconi 146, 00146 Rome, Italy. Tel.: +39-06-55176337; Fax: +39-06-55176321; e-mail: antoccia@bio.uniroma3.it

substrates, such as p53,[13] CDC25C,[14] and Plk1.[15] Chk2 acts in turn as a negative regulator of a mitotic catastrophe in human cells.[9] Very recently, a mitotic catastrophe has been reported to occur in a p53-independent manner and to involve a caspase-2 activation upstream of cytochrome c release, followed by caspase-3 activation and chromatin condensation.[9] By contrast, in tumor cells mitotic catastrophe induced by microtubule interfering agents, such as paclitaxel, epothilone B or combretastatin-A4, has been reported to be a caspase-independent process.[16–19] These results are strengthened by the observation that the inhibition of effector caspase activation does not necessarily protect against cell death. In fact, an alternative apoptotic pathway, referred to as "apoptosis-like", has recentely been uncovered by pan-caspases inhibitors and in caspase mutated cell lines.[2,3,20] Mitochondrial alterations are involved even in an "apoptosis-like" process. In fact, AIF release promotes caspase-independent formation of large chromatin clumps, whereas oligonucleosomal DNA fragments are generated only when caspase-activated DNase CAD is activated.[1,21] In addition, the electron microscope analysis revealed that the biochemical differences between "classical apoptosis" and the "apoptosis-like" are associated with distinctive morphological ultrastructural features, particularly concerning the shape and degree of chromatin condensation.[2,22]

Much recent experimental evidence points to lysosomal proteases, such as cathepsins, calpains and granzymes,[2,3,23] as mediators of caspase-independent cell death. In non-small cell lung cancer cells microtubule stabilizing agents have been shown to trigger the disruption of lysosomal membranes and the release and activation of cathepsin B, while the enzyme inhibition prevents aberrant mitoses.[19]

DZ (Diazepam) is a benzodiazepine and the active constituent of several sedative drugs.[24] At the cellular level, DZ has been reported to inhibit centrosome separation at prophase, leading to monopolar mitotic spindle in human primary fibroblasts.[25] Furthermore, DZ acts as an aneuploidy-inducing agent in both human and hamster cultured cells.[26–29]

Here, we report direct evidence that in HeLa cells abnormal chromosomal segregation caused by impairment of centrosome functionality may lead to a mitotic catastrophe, as a consequence of caspase-independent mechanisms. By contrast, primary human fibroblasts appear to be resistant to DZ-induced cell death.

Materials and methods

Cell cultures and DZ-treatment

Human primary fibroblasts (HFFF2), supplied by the ECACC General Cell Collection, and human epitheloid carcinoma cervix cells (HeLa) were maintained in D-MEM with 10% (v/v) fetal calf serum, 1% (v/v) L-glutamine and antibiotics (all from Gibco, Paisly, UK). Cells were grown in a 5% CO_2 atmosphere at 37°C. Forty-eight h before experiments, 200,000 cells were seeded in 35 mm Petri dishes (Falcon, Becton Dickinson, Franklin Lakes, NJ, USA) containing sterile glass coverslip. DZ (Salars, Como, Italy) was freshly prepared in DMSO (dimethyl sulfoxide) prior to each experiment at a 100-fold concentration. Cells were treated with 281 μM DZ for 12 h whereas control cultures received 1% (v/v) DMSO. Caspase-2 inhibitor Z-VDVAD-FMK (carbobenoxy-Val-Ala-Asp-[O-methyl]-fluomethylketone) and Caspase 3/7 inhibitor (5-[(S)-(+)-2-(Methoxymethyl)pyrrolidino]sulfonylisatin) (both from Calbiochem, La Jolla, CA, USA) were used at concentration 100 μM and 25 μM respectively dissolved in DMSO.

Mitotic arrest

Cells were treated for different times with 281 μM of DZ or 5 μM colchicine (Sigma-Aldrich, St. Louis, MO, USA), then fixed in 3:1 methanol:acetic acid for 30 min and stained with 5% (v/v) Giemsa. The mitotic index was calculated by scoring mitotic figures in a total of 1000 cells per experimental point/experiment in repeated experiments.

Immunofluorescence staining of centrosome and mitotic spindle

Cells were fixed in absolute methanol for 10 min and in acetone for 20 sec at −20°C. After washing with PBS, cells were incubated in a humid chamber for 1 h at 37°C with a non-diluted mouse anti-γ-tubulin antibody (Sigma-Aldrich). Then, slides were rinsed in 1% (w/v) BSA/PBS and incubated for 1 h at 37°C with a diluted 1:15 FITC-conjugated secondary anti-mouse antibody (Vector Laboratories, Burlingame, CA, USA) in 2% (w/v) BSA/PBS. After extensive washing in 1% (w/v) BSA/PBS cells were kept for 1 h in the presence of a diluted 1:50 mouse anti-α-tubulin antibody (Sigma-Aldrich,). Cells were then incubated for 1 h at 37°C with a 1:15 anti-mouse secondary antibody conjugated with Texas Red (Amersham Biosciences, Buckinghamshire, England). DNA was counterstained for 10 min with 0.2 μg/ml DAPI (4′,6′-diamidino-2-phenylindole) (Sigma-Aldrich) and slides mounted with an anti-fade solution (Vectaschield; Vector Laboratories).

At least 100 mitotic figures were scored for each experiment to assess the percentage of monopolar and bipolar mitotic spindles in repeated experiments.

A fluorescence microscope Axiophot (Zeiss, Gottingen, Germany) was used and images were captured with a

Cooled Charged Device (CCD camera) and re-elaborated with an appropriate program (Adobe Photoshop 7.0).

Transmission electron microscopy

Control and DZ-treated cells, grown in to near confluence, were harvested, centrifuged at 1000 rpm for 5 min and fixed with 2.5% (v/v) glutaraldehyde in 0.1 M cacodylate buffer pH 7.2, at room temperature for 1 h. After post-fixation with OsO4 1% (v/v) in cacodylate buffer pH 7.2, at room temperature for 1 h, cells were dehydrated through graded ethanol concentrations with propylene oxide final dehydration. Samples were embedded in Epon 812 (Electron Microscopy Science, Fort Washington, U.S.A). Ultrathin sections, obtained with a LKB ultramicrotome (Ultratome Nova), were stained with uranyl acetate and lead citrate and examined with a Philips 208S electron microscope.

Mitochondrial function and integrity

Changes in the mitochondrial membrane potential (Ψ m) were analyzed using JC-1 (JC-1,5,5′,6,6′-tetrachloro-1,1′,3,3′ tetraethylbenzimidazolylcarbocyanine iodide) (Molecular Probes, Eugene, OR, USA). This cyanine dye accumulates in the mitochondrial matrix under the influence of the Ψm and forms JC-1 aggregates which have characteristic absorption and emission spectra. JC-1 changes colour from green to orange as membrane potentials increase. Reversible formation of JC-1 aggregates causes shift of emitted light from 530 nm to 590 nm.[30]

For flow cytometric analysis, $5{\cdot}10^5$ trypsinized cells were washed with cold medium, then resuspended in 500 μl of medium and incubated with 10 μg/ml of JC-1 for 10 min at 37°C before analysis. Biparametric fluorescence emissions were analyzed by Galaxy flow cytometer (Dako, Glostrup, Denmark).

For microscopic fluorescence analysis, slides were washed once with cold medium and then incubated with 10 μg/ml of JC-1 in 1 ml of medium for 10 min at 37°C. As a positive control for reduction of Ψm, parallel cell cultures were treated with 45 μM of the K^+ ionophore valinomycin (Molecular Probes).

Immunofluorescence staining for activated caspase-3 and caspase-inhibitor treatment with FITC-VAD-FMK (fluorescein-isothiocyanate-Val-Ala-Asp-[O-methyl]-fluoromethylketone)

For immunofluorescnce staining for active caspase-3 cells were fixed in 3% (w/v) paraformaldehyde/PBS for 20 min at 4°C. After 3 washing with TBS-T (tris-buffered saline-tween) (50 mM Tris-HCl pH 7.4, 150 mM NaCl, 0.1% Tween) cells were kept for 1 h with blocking buffer (5% Normal Goat Serum in TBS-T) at room temperature and then incubated overnight at 4°C in a humid chamber with of a diluited 1:100 rabbit anti-cleaved caspase-3 antibody (Cell Signaling Technology, Beverly, MA, USA) in 5% (w/v) BSA/TBS-T. Slides were rinsed in TBS-T and incubated for 1 h at RT with a diluted 1:60 FITC Alexa secondary anti-rabbit antibody (Molecular Probes) in 5% (w/v) BSA/TBS-T. DNA was counterstained with DAPI and slides mounted with an anti-fade solution.

At least 100 apoptotic figures per experiment, based on morphological parameters, were scored to assess the percentage of cells positive or negative to the staining.

To determine caspase activation, treated cells were incubated for 20 minutes at 37°C with 10 μM of the caspases inhibitor FITC-VAD-FMK (Promega, Madison, WI, USA) which binds selectively to active caspases. Then cells were fixed in buffered formalin for 30 minutes at room temperature. The slides were rinsed with PBS, DNA was counterstained for 10 min with 0.2 μg/ml DAPI and slides mounted with an anti-fade solution. Images were captured as reported above.

The role of caspases in DZ-induced aberrant mitoses was analyzed by incubating HeLa cells for 12 h in the presence of DZ alone or in combination with 50 or 100 μM Z-VAD-FMK (carbobenoxy-Val-Ala-Asp-[O-methyl]-fluomethylketone)(Promega) dissolved in DMSO. Cells were fixed in 3:1 methanol:acetic acid for 30 min and stained with 5% (v/v) Giemsa. The mitotic index was calculated by scoring mitotic figures in 2000 cells per experimental point, whereas the frequency of aberrant mitosis was scored in 200 mitotic figures.

Protein extraction and immunoblotting

Non aderent and aderent cells were washed on ice in cold PBS, collected using a scraper, centrifuged for 10 min at 1000 rpm, then the pellet was lysed for 30 min on ice in 40 μl of extraction buffer solution (20 mM Tris HCl pH 8.0, 137 mM NaCl, 10% (v/v) glycerol, 1% (v/v) NP-40, 10 mM EDTA, 1 μg/ml of aprotinin, 1 μg/ml pepstatin, 1 μg/ml and leupeptin, 1 mM orthovanadate, and 2 mM PMSF) or in nuclear protein extraction buffer according to the procedure of Dignam *et al*.[31] Protein concentration was evaluated with a Micro BCA protein assay (Pierce, Rockford, IL, USA) as follows. Briefly, 25 μg of soluble proteins were boiled for 5 min in SDS loading buffer and separated by electrophoresis on a 7% or 12% (w/v) SDS polyacrylammide gel and transferred to a polyvinylidene difluoride membrane (Millipore, Bedford, MA, USA). The efficiency and homogeneity of running and transfer were evaluated using Comassie Blue and Ponceau Red, respectively. Blotted filters were blocked for 30 min in 5% (w/v) skim milk at RT and then incubated over/night with 1 μg/ml antibody anti-Bax (Santa Cruz Biotechnology,

Santa Cruz, CA, USA), PARP (poly-(ADP-ribose) polymerase) (Roche Applied Science, Penzberg, Germany), α-tubulin (Santa Cruz Biotechnology), caspase-9, caspase-3, caspase-6 and caspase-8 (Cell Signaling Technology) activated antibodies.

Filters were then incubated for 1 h at 37°C with secondary anti-mouse or anti-rabbit antibodies (Amersham Biosciences) diluted 1:2000 in skim milk. The antibody reaction was checked by the enhanced chemioluminescence detection procedure according to the manufacturer's instructions (Amersham Biosciences).

Fluorescein-FragEL™ DNA fragmentation analysis

Apoptosis was analysed by the *in situ* Fluorescent-FragEL™ DNA fragmentation kit (Oncogene Research Products, San Diego, CA, USA). Briefly, both control and DZ-treated cells were fixed in 4% (w/v) paraformaldehyde/PBS for 10 minutes at room temperature and rehydratated. Slides were then permeabilized with 20 μg/ml of proteinase K for 5 min at room temperature. After 2 washes in TBS (20 mM Tris pH 7.6, 140 mM NaCl), slides were then equilibrated in TdT (terminal deoxynucleotidyl transferase) equilibration buffer for 30 min at room temperature, then the TdT Labeling Reaction Mixture (TdT enzyme diluted 1:20 in Fluorescein-Fragel TdT Labeling Reaction Mix) was added. Slides were washed in TBS and mounted with Fluorescent-Fragel mounting media.

Cytofluorimetric analysis of subdiploid (subG1) DNA peak

Apoptosis was assessed by DNA fluorescence flow cytometric profiles. Cells detached from plates were washed two-fold in PBS, then resuspended in 1 ml of fluorochromic solution containing 0.05 mg/ml PI (propidium iodide), 0.1% sodium citrate and 0.1% Triton X-100 and then placed at 4°C in the dark overnight before the flow-cytometric analysis. The fluorescence of DNA of isolated nuclei (PI fluorescence) was analyzed by Galaxy flow cytometer (Dako , Glostrup, Denmark) and the percentage of apoptotic nuclei (subdiploid DNA peak in the DNA fluorescence histogram) was calculated using WinMDI software v. 2.8 (Joe Trotter).

Results

DZ arrests cells at a prometaphase stage

Treatment of HFFF2 primary fibroblasts with DZ for 12 h induced a 1.4-fold-increase of mitotic index as compared with untreated cultures, whereas such increase was of 4.6-fold in HeLa cells (Figure 1). To ascertain whether cells were in a growing phase and displayed an efficiency in mitotic block, other cultures were treated in parallel with 5 μM colchicine. Cytofluorimetric experiments with an antibody specific for the phosphorylated form of histone-H3 gave similar results (not shown), indicating that DZ was more effective in HeLa than in primary cells.

Figure 1. Effect of 281 μM DZ and 5 μM colchicine on mitotic index (M.I.). The M.I. of treated cells is represented as fold-increase over the M.I. scored in untreated cultures.

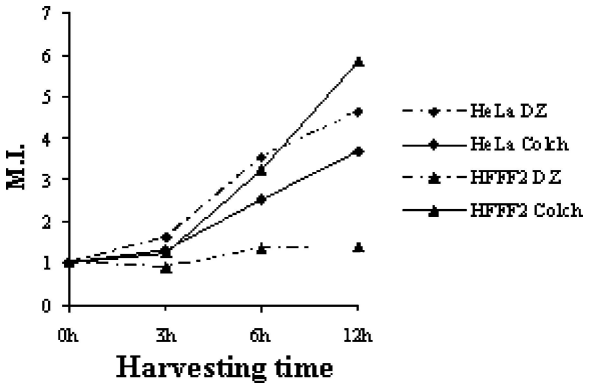

We then looked at the morphology of mitotic arrested cells processed for Giemsa staining, indirect immunofluorescence and TEM (trasmission electron microscopy) (Figure 2). In particular to investigate possible alterations in the mitotic spindle and centrosomes, specific antibodies were used, namely, anti-α-tubulin for mitotic spindle microtubules and anti-γ-tubulin, directed to the pericentriolar material of centrosomes.[32]

Figure 2 shows representative examples of DZ-induced mitotic figures in HeLa cell cultures, as revealed by Giemsa staining (a–c), α- and γ-tubulin double immunofluorescence (d–f) and TEM (g–i). Normal metaphases showing a bipolar arrangement of mitotic spindle and chromosomes gathered to the equatorial plane were observed in control untreated cells (Figures 2a, d and g). DZ treatment produced monopolar metaphases (Figures 2b, e and h); as revealed by the γ-tubulin immunolocalization, centrosomes were duplicated but still unseparated, while anti-α-tubulin revealed monopolar spindle (Figure 2e, large arrow). The peculiar arrangement of chromosomes and the central position of unseparated centrosomes is revealed in further detail by TEM analysis (Figure 2h). In fibroblast cultures, DZ induced monopolar metaphases with unseparated centrosomes in more than 98% of cells arrested in mitosis.

In spite of the 12h-DZ-treatment, some HeLa cells progressed through mitosis, giving rise to mitotic failure events (Figures 2c, f and i). In fact, many of the aberrant metaphases showed separated centrosomes, bipolar α-tubulin-stained mitotic spindle and masses of chromatin arranged outside the equatorial plate. In such mitoses, displaced chromosomes were readily detected by

Figure 2. Treatment with DZ induces the formation of abnormal metaphases in HeLa cells. Control cells (a, d, g) and cells treated for 12 h with 281 μM DZ (b, c, e, f, h, i) were stained with Giemsa, immunostained with antibodies against γ-tubulin (red) and α-tubulin (green) or analyzed by transmission electron microscopy. DNA was counterstained with DAPI (blue). Control cells showed a bipolar spindle with γ-tubulin localized at poles and DNA aligned in metaphase plate (a,d,g). After treatment with DZ, monopolar spindles with centrosomes showing various degrees of separation (b, e, h) and aberrant bipolar spindles with masses of chromatin displaced outside the equatorial plate, but connected to the spindle poles, were observed (c, f, i). Classification and frequency of the scored prometaphases into four categories based on the immunofluorescence staining with antibodies against γ- and α-tubulin and DNA counterstainig with DAPI in DZ-treated HeLa and HFFF2 (l). Bars: $\pm$SE.

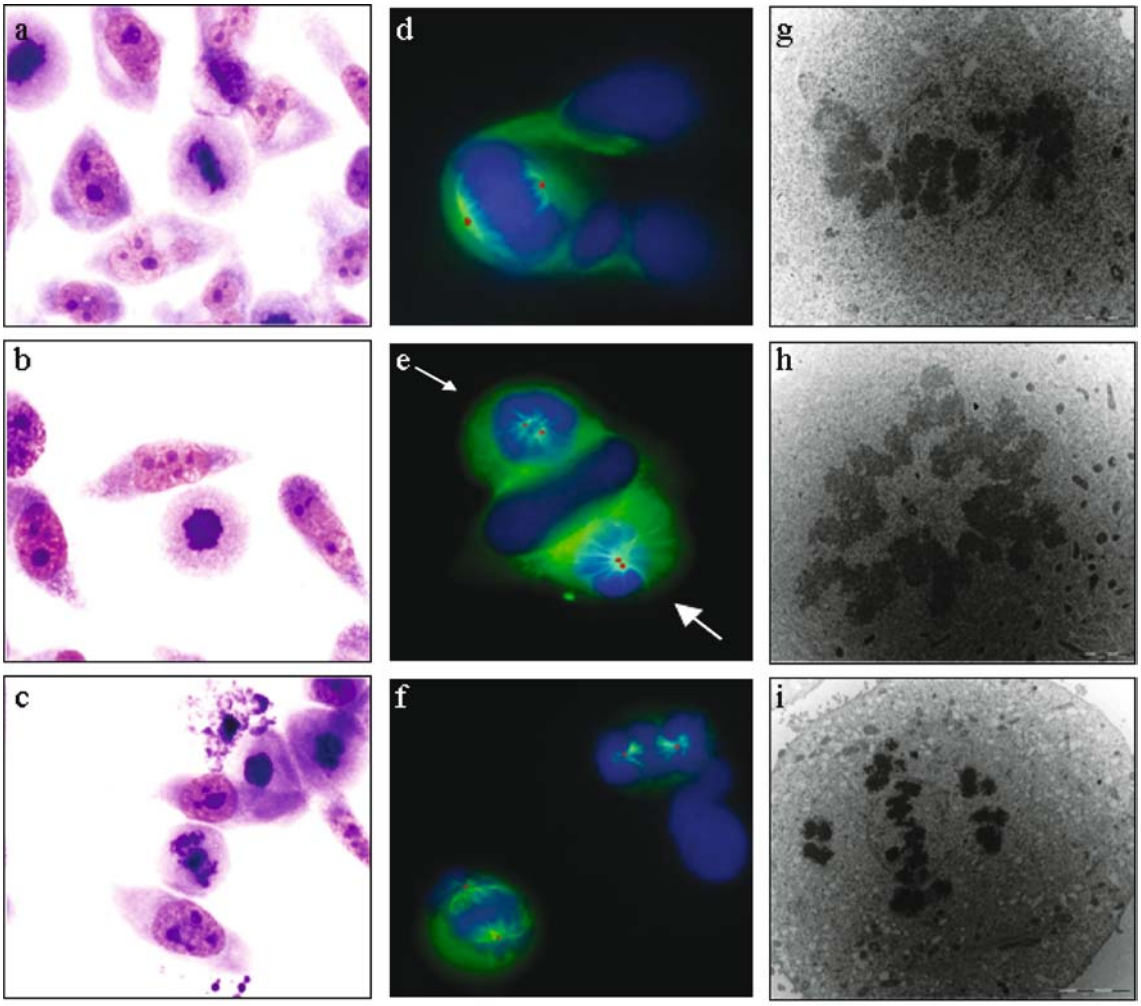

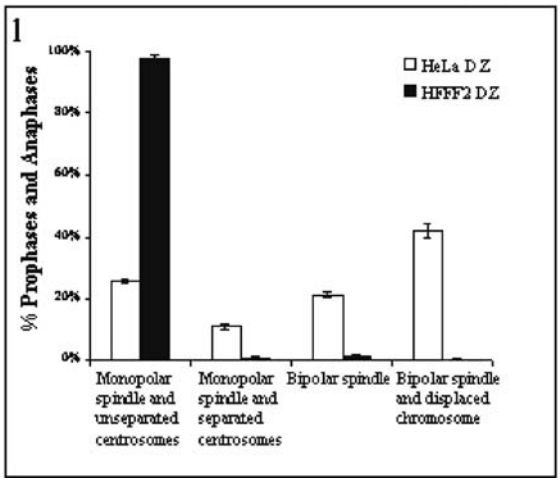

Figure 3. Western blot with Bax antibody on whole protein extracts from HeLa and HFFF2 cells treated either for 12 h with 281 μM DZ or for 3 h with 2 μM staurosporine (STS). Equal loading of proteins was ascertained with an antibody directed to α-tubulin.

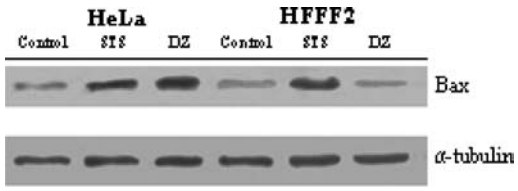

TEM (Figure 2i).

In Figure 2l, the distribution of the different types of mitotic figures, as classified after staining with α and γ-tubulin antibodies, is reported. Values obtained in treated samples were normalized on figures scored in untreated cultures. As stated before, DZ-treated primary fibroblasts showed nearly 100% metaphases with unseparated centrosomes, whereas in HeLa cells they represented only 26% of the scored mitotic figures. In HeLa cells, prometaphases with various degrees of centrosome separation (11%) and mitotic cells with a bipolar spindle (21%) were also observed. In addition, 42% of the analyzed mitoses showed a bipolar mitotic spindle with few-to-many chromosomes localised near the poles and thus displaced from the remaining chromosomes at the equatorial plane. Cells bearing these features were interpreted as undergoing mitotic catastrophe.

DZ induces alterations in MMP

Mitochondrial alterations induced by DZ in HeLa cells were accompanied by accumulation of Bax protein, as evaluated by immunoblot analysis, whereas levels of the protein were unchanged in HFFF2 fibroblasts. Staurosporine, a well known agent inducing apoptosis, was used as a positive control (Figure 3).

After 6 or 12 h of DZ-treatment, both HeLa cells and fibroblasts were loaded with JC-1, a specific indicator of mitochondrial membrane potential (Ψm). DZ treatment induced perturbations in the function of mitochondrial membranes, as indicated by the orange to green colour switch in a great number of HeLa cells; such an effect was not observed in DZ-treated primary fibroblasts. Furthermore, incubation in the simultaneous presence of DZ and Z-VDVAD-FMK, a specific inhibitor of caspase-2, did not prevent mitochondrial memebrane depolymerization. A loss of MMP was observed in both HeLa and HFFF2 cells after exposure to staurosporine (Figure 4c, f).

Flow cytometric quantitative analysis performed on HeLa cells after JC-1 labelling, clearly showed that DZ induces alterations in the mitochondrial membranes 7.8-fold as compared to untreated cultures (Figures 4l and m); staurosporine was even more potent (13.6-fold) (Figure 4n). The ionophore valinomycin was used as a positive control for the staining assay, showing 98% of JC-1 positive cells (Figure 4o).

Figure 4. Fluorescence staining with JC-1 of untreated and DZ-treated or staurosporine-treated HeLa (a, b, c) and HFFF2 fibroblasts (d, e, f). HeLa cells treated with Z-VDVAD-FMK, an inhibitor of caspase-2, alone (g) or in combination for 12 h with DZ (h). Cytofluorimetric quantification of JC-1 staining HeLa cells. Bivariate plots of orange (FL2) versus green (FL1) fluorescence as an estimate of mitochondrial membrane potential (Ψm). Values indicate percentages of depolarized mitochondria. Untreated controls (i), 281 μM DZ 6 h (l) and 12 h (m), 2 μM staurosporine 3 h (n) and 45 μM valinomycin 10 min (o).

Changes in the mitochondrial membrane potential induced by DZ treatment were accompanied by remarkable alterations in the mitochondrial ultrastructure. In fact, while untreated HeLa cells showed well preserved mitochondria with well defined and parallel cristae and a homogeneous matrix (Figure 5), after 6 h of DZ treatment, most mitochondria displayed irregular shapes and dilated cristae (Figure 5). These modifications were even more evident after treatment for 12 h: mitochondria underwent fragmentation with vacuolized cristae in a highly condensed matrix (Figure 5).

DZ induces apoptosis through a caspase-independent mechanism

Since mitotic catastrophe has been reported by some authors as a caspase-3-independent process,[18] we used specific antibodies against active caspases-9, -8, -3, -6 to ascertain the role of these enzymes in DZ-induced HeLa cell death. Western blot analysis of time-course experiments

Figure 6. DZ-treated HeLa cells follow caspase-9, caspase-3, caspase-6 and caspase-8-independent apoptosis. Western blot analysis of whole protein extracts from HeLa cells treated either for 4, 8, and 12 h with 281 μM DZ carried out with antibodies directed to cleaved caspase-9, -3, -6 and -8. As positive controls, cells were treated 3 h with 1 μM and 2 μM staurosporine, or 5 h with 10 nM α-TNF. Equal loading of proteins was probed with α-tubulin antibody (a). Examples of apoptotic HeLa cells as induced by DZ (b) and staurosporine (c) both showing DNA condensation and fragmentation and negative or positive to immunofluorescence staining with an antibody against activated caspase-3. Percentage of caspase-3 positive and negative apoptotic cells as observed after treatment with DZ or staurosporine (d). Caspase activation occurs only in staurosporine-treated cells (e,f,g) as evaluated by incubation with FITC-VAD-FMK, which binds to activated caspases. Effect of a Z-VAD-FMK inhibitor on aberrant mitosis induced by DZ (h). Cells were treated for 12 h with 281 μM DZ alone or in combination with 50 or 100 mM Z-VAD-FMK. Bars: $\pm$SE.

Figure 4.

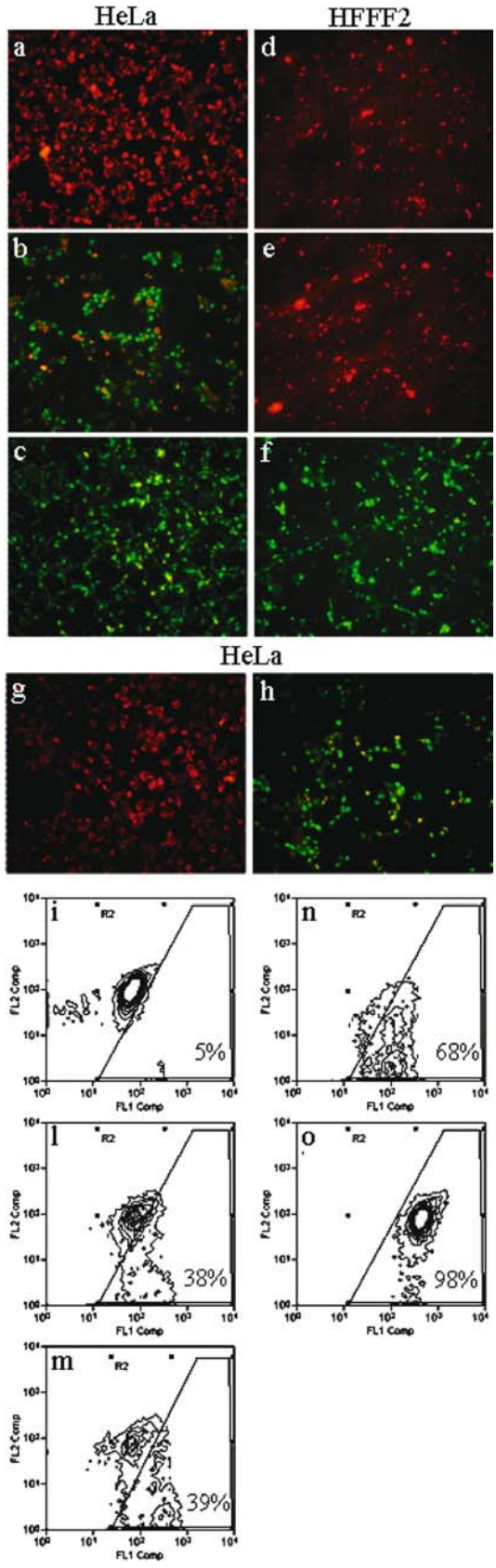

Figure 6.

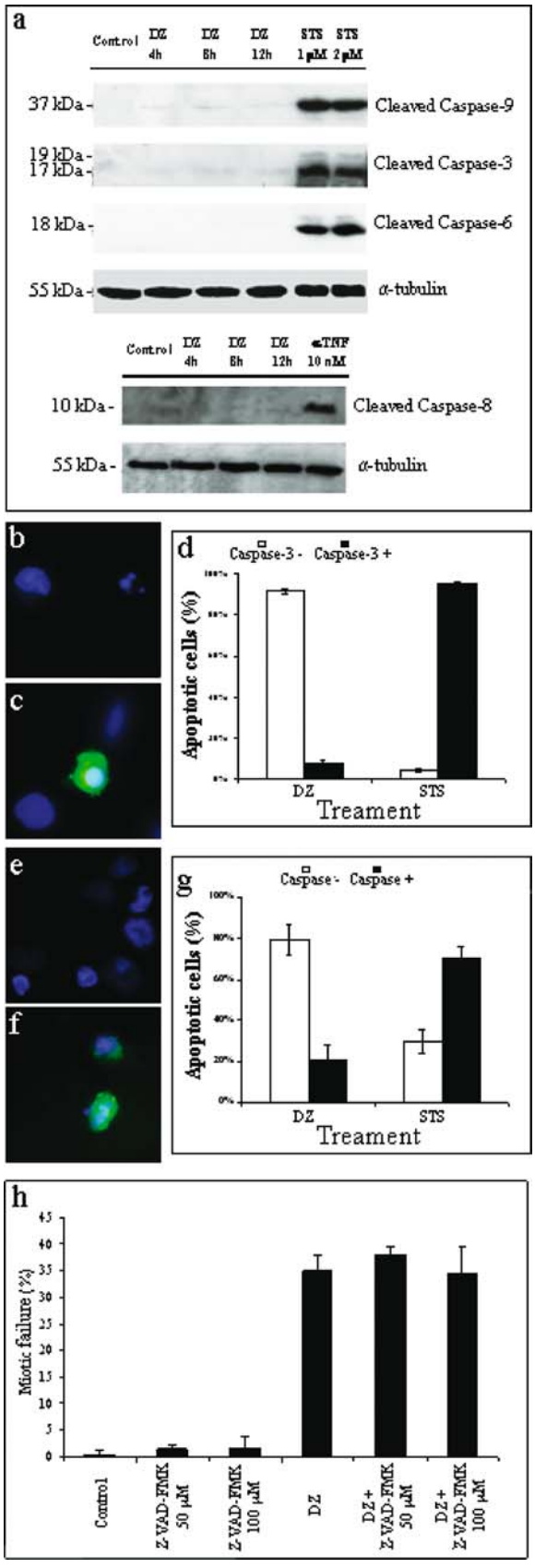

Figure 5. Transmission electron microscopy observations of untreated (a) and DZ-treated HeLa cells for 6 and 12 h (b and c, respectively).

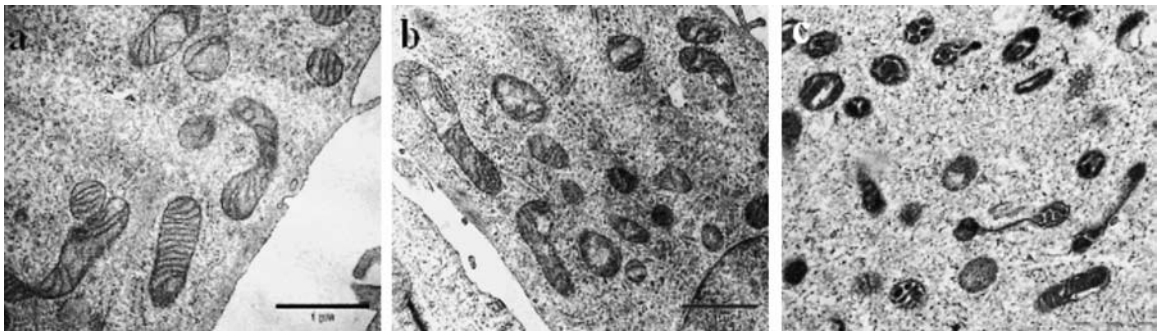

indicated that DZ leads to reduced activation of caspase-9, whereas caspase-3 was almost undetectable, as compared to staurosporine-treatment (Figure 6a). Furthermore, we found no activation of caspase-6 and caspase-8 after DZ-treatment (Figure 6a).

Consistent with these data, staurosporine induced a high proportion of caspase-3 immunoreactive apoptotic cells, whilst only 8% of DZ treated cells were positive. In addition, 20 and 70% of DZ and staurosporine-treated cells, respectively, were stained by FITC-VAD-FMK, a compound which binds exclusively to activated caspases (Figure 6). In agreement with these observations, neither the mitotic index nor the frequency of aberrant mitosis induced by DZ was affected by incubation with the general caspase inhibitor Z-VAD-FMK (Figure 6).

Furthermore, the understanding of mechanisms leading to cell death might well benefit from the analysis of higly specific morphological markers. TEM analysis of HeLa cells treated with either DZ or staurosporine revealed consistent differences in their morphological features. The morphological changes of the cells treated with staurosporine showed signs of "classical" apoptosis, including chromatin condensation in compact and apparently simple geometric (globular, crescent-shaped) figures, cytoplasmic shrinkage, zeiosis, and formation of apoptotic bodies with nuclear fragments (Figure 7). By contrast, in DZ treated cells chromatin condensation was less prominent and complete (geometrically more complex and lumpier shapes), and cytoplasm vacuolization was a common finding (Figure 7). These features are recognised as typical hallmarks of the so-called "apoptosis-like" cell death.[2]

Figure 7. Differences between classical apoptosis induced by staurosporine (a) and "apoptosis-like" cell death induced by DZ (b).

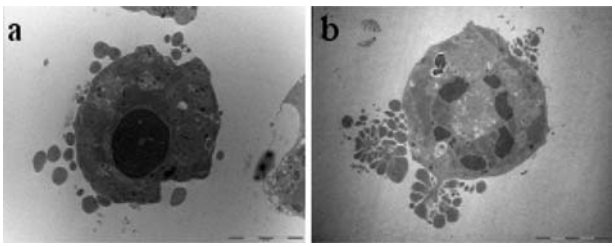

Hallmarks of apoptosis other than caspase activation were detected in DZ-treated cells

Immunoblot analysis performed with a PARP antibody clearly indicated the presence of the 89 kDa apoptotic-associated fragment after exposure of HeLa cells to either DZ or staurosporine. However, the intensity of the signal for the 89 kDa fragment was stronger in staurosporine than in DZ-treated cells (Figure 8). Apoptosis was demonstrated also by DNA fluorescence flow cytometric profiles. DZ was able to induce apoptosis in HeLa cells, however the extent of such induction was lower compared to that obtained by means of TUNEL assay (Figure 8).

Furthermore, committment to apoptosis was confirmed by TUNEL, a specific assay for DNA interucleosomal cleavage. Both DZ and staurosporine were able to induce DNA fragmentation in HeLa cells (Figure 8f, g). The quantitative analysis as performed by TUNEL assay in HeLa cell cultures showed that DZ and staurosporine induced about 30 and 73% apoptotic cells, respectively (Figure 8h). No modulation of DZ-induced DNA fragmentation was detected in case of combinated incubation with a caspase-2 (Z-VDVAD-FMK) and a caspase 3/7 specific inhibitor (Figure 8).

Untreated and DZ-treated HFFF2 were negative to the immunofluorescent staining for DNA fragmentation, whereas positive staining was detected in HFFF2 treated with staurosporine (Figure 8o, p, q).

Discussion

In this paper, we show that the centrosome-separation inhibitor DZ induces cell death by a mitotic catastrophe casapase-3-independent mechanism in HeLa cells but not in primary fibroblasts.

Figure 8. Western blot analysis of PARP cleavage on nuclear protein extracts. The presence of signal at 116-kDa indicates uncleaved protein, whereas the 89-kDa signal indicates the apoptotic-cleaved protein. Cells were treated for 12 h with 281 μM DZ or 3 h with 2 μM staurosporine (a). DNA fluorescent cytometric profiles of untreated HeLa cells (b) or treated either for 12 h with 281 μM DZ (c) or for 3 h with 2 μM staurosporine (d). In the panel are reported the percentages of apoptotic nuclei (cells with a subdiploid content of DNA). DZ induces apoptosis only in HeLa cells as evaluated by means of Fluorescent-FragEL™ DNA fragmentation kit. Immunofluorescent staining of untreated HeLa cells (e) or treated either for 12 h with 281 μM DZ (f) or for 3 h with 2 μM staurosporine (g). Percentage of HeLa apoptotic cells as measured by scoring for cells positive to the immunofluorescent staining (h). Cells treated with 100 μM caspase-2 (i) and 25 μM caspase 3/7 inhibitors (m) or in combination with DZ (l,n). Primary fibroblasts HFFF2 were resistant to DZ-induced apoptosis. Untreated fibroblasts (o) and cells treated with either DZ (p) or staurosporine (q). Bars: ±SE.

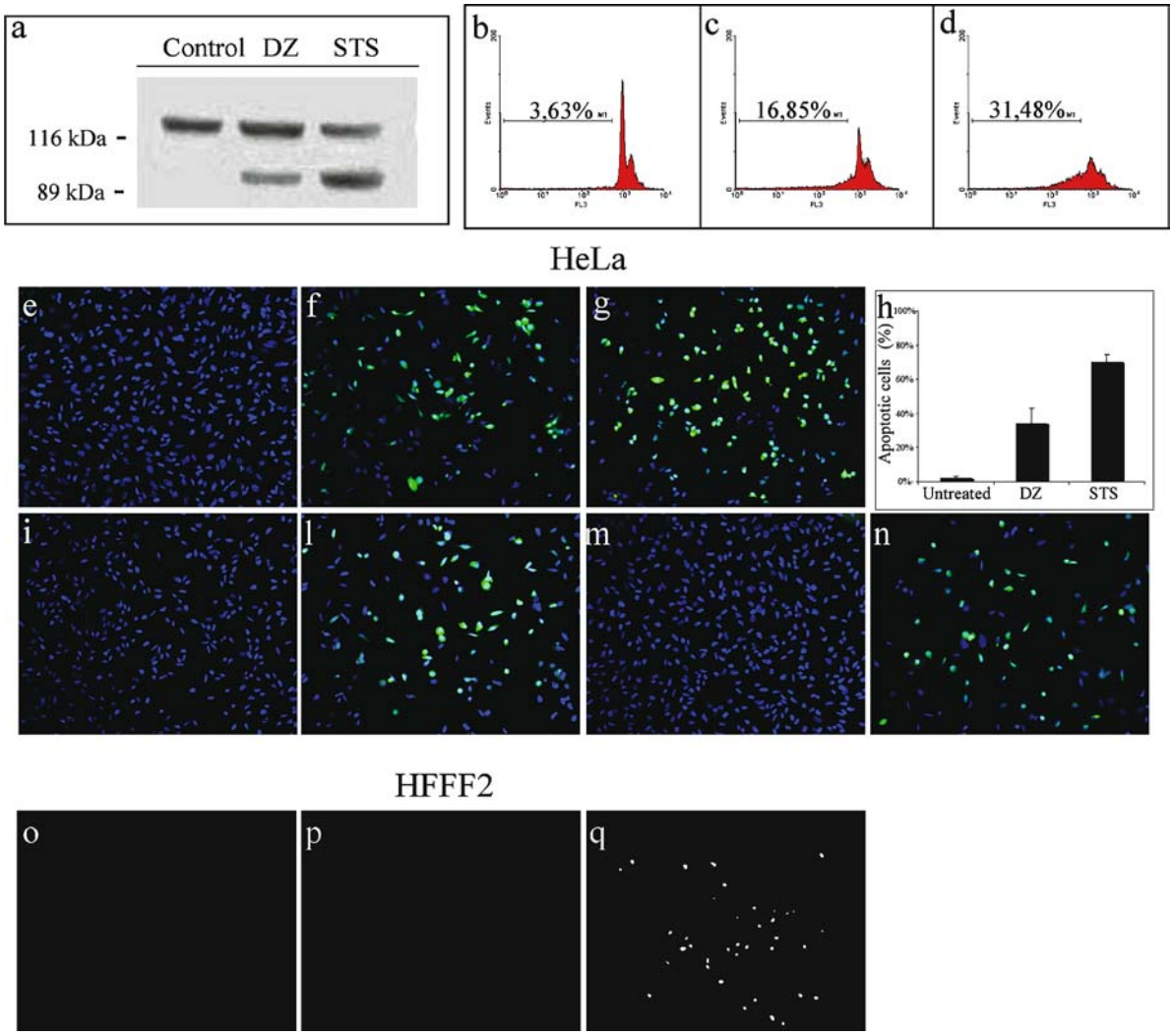

By interfering with centrosome splitting in the prophase-to-prometaphase transition, DZ is able to act as a mitotic arrestant. However, while a consistent and comparable mitotic accumulation has been obtained in several tumour cell lines treated with either DZ or colchicine, DZ acts as a poor mitotic arrestant only in HFFF2 primary fibroblasts and lymphocytes (present results;[28]). This may indicate either that cells are delayed in phases that preeced mitosis or that DZ is less active in primary cells. However, those cells reaching mitosis are strongly arrested at the prometaphase stage with a monopolar spindle and unseparated pairs of centrosomes, as previously reported by Andersson *et al*.[25] Contrastingly, HeLa cells and other five tumour lines investigated (MCF-7, Hep2, SiHa, Me180 and HepG2; data not shown), display a high proportion of mitosis with various degrees of centrosome separation after DZ treatment. More than half of mitotic cells become transiently arrested at the prometaphase stage and then attempt to go through mitosis without the completion of proper chromosome congression. As a result of treatment, mitotic failure occurred as shown by the massive presence of markedly irregular mitosis with masses of chromatin displaced from the equatorial plate.

Moreover, in our experiments, we observed neither anaphases nor cells with a polyploid nucleus. These findings support the notion that cells fail to progress from prometaphase to metaphase, that is before a proper chromosome aggregation, and die before attempting metaphase to anaphase transition.

The present results are reminiscent of those produced by a dominant-negative Plk1, which has been reported to affect centrosome separation and induce mitotic catastrophe in HeLa cells but not in Hs68 fibroblasts and normal human mammary epithelial cells.[7,33] It is interesting to remark that the kinase activation of Cdk1 was reported to be blocked by the dominant-negative Plk1 in both normal epithelial cells and in tumour lines regardless of whether they underwent a mitotic catastrophe.[7] Similarly, we detected a far higher amount of Tyr15-phosphorylated Cdk1 after DZ treatment (data not shown), which corresponds to the inactive form.[34] This finding seems to suggest that the mitotic failure is not attributable to a lack of dependence for DZ in activating Cdk1. Contrastingly, combretastatin-A4, an inhibitor of microtubule assembly,[35] induces a mitotic catastrophe independent of Cdk-1 phosphorylation in leukemia cells,[18] indicating that the biochemical markers responsible for this type of cell death may be cell type-dependent.

It is well known that the proper attachment of kinetochores at the mitotic spindle is monitored by the spindle assembly checkpoint driven by the APC (anaphase-promoting complex).[36] Checkpoint proteins as MAD2 (mitotic arrest deficient) inhibit the APC when chromosomes are unattached or not bipolarly attached to the mitotic spindle, a condition that fails to generate tension at the kinetochore.[37] In this respect, agents affecting centrosome separation, as DZ or monoastrol (an inhibitor of the Eg5 kinesin),[38,39] determine a syntelic attachment (paired kinetochores may capture microtubules coming from the same spindle pole), a condition that may well activate the spindle checkpoint.[39] Since a mitotic checkpoint deficiency has been reported in several cell lines,[40,41] we checked this possibility by means of a treatment with classical anti-microtubule depolymerizing agents: both cell types underwent a mitotic block after colchicine, showing an efficient checkpoint.

It has been suggested that a mitotic arrest triggers a mitotic spindle checkpoint, which somehow, maybe through caspase-2 and the Bcl-2 family proteins, is likely to affect the mitochondrial permeability, as well as the release of proapoptotic factors into cytosol, the activation of caspases, and finally the execution of mitotic catastrophe.[6,42,43] Recently, it has been shown that mitotic catastrophe induced by Chk2 inhibition involves primary activation of caspase-2 upstream of mitochondrial membran modifications.[43] In our experiments we find neither loss of MMP nor reduction of DNA fragmentation in DZ-treated cells co-incubated with a specific inhibitor of caspase-2, suggesting that mitotic catastrophe activated by mitotic-interfering agents may follow a different pathway.

Despite the absence of caspase-2 activation, Bax, which by interacting with other Bcl-2 family members regulates the release of proapoptotic factors, was induced after DZ treatment solely in HeLa cells. Furthermore, we found that mitochondria underwent marked changes: they were collapsed and showed almost complete disorganization of cristae, whereas the mitochondria from untreated samples appeared elongated, oval-shaped and with dense cristae. These results indicate that in HeLa cells, DZ triggers irreversible mitochondrial morphological and ultrastructural alterations accompanied by a loss of MMP, as shown by JC-1 staining.[30]

Beside mitotic alterations on mitochondrial morphology and functionality, it can be also speculated that such an impairment occurs as the result of DZ binding to PBR (peripheral-type benzodiazepine receptors), which reside in the mitochondrial outer membrane and contribute to permeability transition pores.[44] The cytosolic release of endozepine, the cellular endogenous ligand of PBR, may participate in a positive feedback loop accelerating MMP.[45] Furthermore, apoptosis induced by the anti-CD95 receptor antibody was shown to be enhanced by different ligands of the benzodiazepine receptor in human tumour cells and the combined treatment of DZ and lonidamine was shown to be successfully applied to eradicate glioblastoma.[46,47] Furthermore, the chronic use of DZ has been associated with a more favourable outcome in breast cancer.[48] The difference observed between HeLa and primary cells, may be well explained by the observation that PBR are overexpressed in many tumour types.[49] However, RT-PCR analysis indicated that both cell lines we used expressed detectable and comparable levels of mRNA transcripts for PBR (not shown). In addition, in our experiments the effect of DZ seemed to be restricted to mitotic cells, pointing to a stage-specific effect of the drug, which would not be expected on the basis of the PBR presence only.

As a consequence of the loss in MMP, we found that distinctive markers of apoptosis commitment were displayed only in DZ-treated HeLa cells. Then, PARP cleavage and DNA internucleosomal fragmentation occurred in spite of a very low or absent caspase-9, -8, -6, -3 and -2 activation, thereby suggesting a caspase-independent cell death mechanism. This finding is corroborated by the observation that the frequency of aberrant mitosis was not suppressed by DZ treatment in combination with the pan-caspase inhibitor Z-VAD-FMK, indicating that proteases other than caspases may be involved in perturbation of the proper mitosis. Similarly, this observation is supported by experiments carried out at a cellular level with the pan-caspase inhibitor and specific inhibitors of caspase-2 and of caspase-3/7.

In this regard, downstream differences in the mitotic catastrophe as obtained exposing cells either to spindle depolymerizing and stabilizing agents or to DZ should be emphasized. Several reports have indicated a caspase-dependent apoptosis after treatment with a number of microtubule-targeted anticancer agents, such as paclitaxel.[42] However, using the caspase inhibitors Z-VAD-FMK, other authors failed to prevent a mitotic catastrophe induced by classical spindle poisons or combretastatin-A4, and made the conclusion that such type of cell death is unrelated to caspase activation.[17–19,22]

As reported over the last few years, many cell death mechanisms have been defined as apoptosis-like programmed cell death, driven by an active process dependent on signalling events, not necessarily caused by caspase activation and often of lysosomial origin.[2,3,23,50] For the caspase-dependent and caspase-independent cell death pathways, mitochondria are central stations; in response to apoptotic stimuli, they can also release caspase-independent cell death effectors such as AIF and endonuclease G.[51] Together with the lack of caspase-3 activation, the morphological features obtained by TEM analysis of DZ-treated cells revealed features that were observed in caspase-3 deficient cells MCF-7 induced to cell death.[2,52] In agreement with our observations, it has been reported that caspase-3 deficiency does not affect Bax-induced level of PARP cleavage.[20]

Recently, the role of lysosomes and lysosomal enzymes in initiation and execution of the apoptotic program has been shown in several models.[50] As a result, non-caspase proteases such as cathepsins appear to be important regulators in caspase-independent apoptosis, as recently demonstrated for the role of cathepsin-B in mediating a mitotic catastrophe in lung cancer cells.[19]

Conclusions

In conclusion, the present results indicate that, by interfering with the proper centrosome separation, DZ is able to induce mitotic catastrophe events in HeLa cells, but not in primary fibroblasts. The drug is capable of activating the mitochondrial pathway, which in turn leads to a caspase independent cell death. The observation that checkpoint defects and mutation in caspase genes are frequently found in tumour cells, points to the relevance of centrosome-interfering agents as a possible tool to eradicate malignancy.

However, further experiments need to better clarify the apoptotic response to benzodiazepine and the cell specificity, in that C6 rat glioma cells have been shown to be resistant to DZ treatment whereas the PBR-ligands, PK 11195 and Ro5-4864 induce in the same cells caspase-3-dependent apoptosis.[53]

Acknowledgments

We are grateful to Prof. P. Ascenzi for critical reading of the manuscript.

References

1. Strasser A, O'Connor L, Dixit VM. Apoptosis signaling. *Annu Rev Biochem* 2000; **69**(2): 17–45.
2. Leist M, Jaattela M. Four deaths and a funeral: From caspases to alternative mechanisms. *Nat Rev Mol Cell Biol* 2001; **2**: 589–598.
3. Jaattela M. Multiple cell death pathways as regulators of tumour initiation and progression. *Oncogene* 2004; **23**: 2746–2756.
4. Hengartner MO. The biochemistry of apoptosis. *Nature* 2000; **407**: 770–776.
5. Shimizu S, Narita M, Tsujimoto Y. Bcl-2 family proteins regulate the release of apoptogenic cytochrome c by the mitochondrial channel VDAC. *Nature* 1999; **399**: 483–487. Erratum in: *Nature* **407**: 767.
6. Mollinedo F, Gajate C. Microtubules, microtubule-interfering agents and apoptosis. *Apoptosis* 2003; **8**: 413–450.
7. Cogswell JP, Brown CE, Bisi JE, Neill SD. Dominant-negative polo-like kinase 1 induces mitotic catastrophe independent of cdc25C function. *Cell Growth Differ* 2000; **11**: 615–623.
8. Sato N, Mizumoto K, Nakamura M, *et al.* A possible role for centrosome overduplication in radiation-induced cell death. *Oncogene* 2000; **19**: 5281–5290.
9. Castedo M, Perfettini JL, Roumier T, Andreau K, Medema R, Kroemer G. Cell death by mitotic catastrophe: A molecular definition. *Oncogene* 2004; **23**: 2825–2837.
10. Swanson PE, Carroll SB, Zhang XF, Mackey MA. Spontaneous premature chromosome condensation, micronucleus formation, and non-apoptotic cell death in heated HeLa S3 cells. Ultrastructural observations. *Am J Pathol* 1995; **146**: 963–971.
11. Ianzini F, Mackey MA. Spontaneous premature chromosome condensation and mitotic catastrophe following irradiation of HeLa S3 cells. *Int J Radiat Biol* 1997; **72**: 409–421.
12. Tsvetkov L, Xu X, Li J, Stern DF. Polo-like kinase 1 and Chk2 interact and co-localize to centrosomes and the midbody. *J Biol Chem* 2003; **278**: 8468–8475.
13. Chehab NH, Malikzay A, Appel M, Halazonetis TD. Chk2/hCds1 functions as a DNA damage checkpoint in G(1) by stabilizing p53. *Genes Dev* 2000; **14**: 278–288.
14. Peng CY, Graves PR, Thoma RS, Wu Z, Shaw AS. Piwnica-Worms. Mitotic and G2 checkpoint control: Regulation of 14-3-3 protein binding by phosphorylation of Cdc25C on serine-216. *Science* 1997; **277**: 1501–1505.
15. Seo GJ, Kim SE, Lee YM, Lee JW, Lee JR, Hahn MJ, Kim ST. Determination of substrate specificity and putative substrates of Chk2 kinase. *Biochem Biophys Res Commun* 2003; **304**: 339–343.
16. Broker LE, Huisman C, Ferreira CG, Rodriguez JA, Kruyt FA, Giaccone G. Late activation of apoptotic pathways plays a negligible role in mediating the cytotoxic effects of discodermolide and epothilone B in non-small cell lung cancer cells. *Cancer Res* 2002; **62**: 4081–4088.
17. Huisman C, Ferreira CG, Broker LE, *et al.* Paclitaxel triggers cell death primarily via caspase-independent routes in the non-small cell lung cancer cell line NCI-H460. *Clin Cancer Res* 2002; **8**: 596–606.

18. Nabha SM, Mohammad RM, Dandashi MH, *et al.* Combretastatin-A4 prodrug induces mitotic catastrophe in chronic lymphocytic leukemia cell line independent of caspase activation and poly(ADP-ribose) polymerase cleavage. *Clin Cancer Res* 2002; **8**: 2735–2741.
19. Broker LE, Huisman C, Span SW, Rodriguez JA, Kruyt FA, Giaccone G. Cathepsin B mediates caspase-independent cell death induced by microtubule stabilizing agents in non-small cell lung cancer cells. *Cancer Res* 2004; **64**: 27–30.
20. Kagawa S, Gu J, Honda T, McDonnell TJ, Swisher SG, Roth JA, Fang B. Deficiency of caspase-3 in MCF7 cells blocks Bax-mediated nuclear fragmentation but not cell death. *Clin Cancer Res* 2001; 7: 1474–1480.
21. Susin SA, Lorenzo HK, Zamzami N, *et al*. Molecular characterization of mitochondrial apoptosis-inducing factor. *Nature* 1999; **397**: 441–446.
22. Volbracht C, Leist M, Kolb SA, Nicotera P. Apoptosis in caspase-inhibited neurons. *Mol Med* 2001; 7: 36–48.
23. Lockshin RA, Zakeri Z. Caspase-independent cell death? *Oncogene* 2004; **23**: 2766–2773.
24. Byck R. Drugs and the treatment of psychiatric disorders. In: Goodman LS, Gilman A, eds *The Pharmacological Basis of Therapeutics*, New York: Edn. Mcmillan. 1975; 189–192.
25. Andersson L., Letho V, Stenman S, Bodley RA, Virtamen I. Diazepam induces mitotic arrest at prometaphase by inhibiting centriolar separation. *Nature* 1981; **291**: 247–248.
26. Lafi A, Parry JM. A study of the induction of aneuploidy and chromosome aberrations after diazepam, medazepam, midazolam and bromazepam treatment. *Mutagenesis* 1988; **3**: 23–27.
27. Antoccia A, Degrassi F, Battistoni A, Ciliutti P, Tanzarella C. *In vitro* micronucleus test with kinetochore staining: Evaluation of test performance. *Mutagenesis* 1991; 6: 319–324.
28. Sbrana I, Di Sibio A, Lomi A, Scarcelli V. C-mitosis and numerical chromosome aberration analyses in human lymphocytes: 10 known or suspected spindle poisons. *Mutat Res* 1993; **287**: 57–70.
29. Izzo M, Antoccia A, Degrassi F, Tanzarella C. Immunofluorescence analysis of diazepam-induced mitotic apparatus anomalies and chromosome loss in Chinese hamster cells. *Mutagenesis* 1998; **13**: 445–451.
30. Cossarizza A, Baccarani-Contri M, Kalashnikova G, Franceschi C. (1993). A new method for the cytofluorimetric analysis of mitochondrial membrane potential using the J-aggregate forming lipophilic cation 5,5′,6,6′-tetrachloro-1,1′,3,3′-tetraethylbenzimidazolcarbocyanine iodide (JC-1). *Biochem Biophys Res Commun* **197**: 40–45.
31. Dignam JD, Lebovitz RM, Roeder RG. Accurate transcription initiation by RNA polymerase II in a soluble extract from isolated mammalian nuclei. *Nucleic Acids Res* 1983; **11**: 1475–1489.
32. Doxsey S. Re-evaluating centrosome function. *Nat Rev Mol Cell Biol* 2001; **2**: 688–698.
33. Lane HA, Nigg EA. Antibody microinjection reveals an essential role for human polo-like kinase 1 (Plk1) in the functional maturation of mitotic centrosomes. *J Cell Biol* 1996; **135**: 1701–1713.
34. Shackelford RE, Kaufmann WK, Paules RS. Cell cycle control checkpoint mechanism and genotoxic stress. *Environ Health Persp* 1999; **107**: 5–11.
35. Woods JA, Hadfield JA, Pettit GR, Fox BW, McGown AT. (1995). The interaction with tubulin of a series of stilbenes based on combretastatin A-4. *Br J Cancer* **71**: 705–711.
36. Wassmann K, Benezra R. Mitotic checkpoints: From yeast to cancer. *Curr Opin Genet Dev* 2001; **11**: 83–90.
37. Wassmann K, Liberal V, Benezra R. Mad2 phosphorylation regulates its association with Mad1 and the APC/C. *EMBO J* 2003; **22**: 797–806.
38. Mayer TU, Kapoor TM, Haggarty SJ, King RW, Schreiber SL, Mitchison TJ. Small molecule inhibitor of mitotic spindle bipolarity identified in a phenotype-based screen. *Science* 1999; **286**: 971–974.
39. Lens SM, Wolthuis RM, Klompmaker R, *et al.* Survivin is required for a sustained spindle checkpoint arrest in response to lack of tension. *EMBO J* 2003; **22**: 2934–2947.
40. Blajeski AL, Phan VA, Kottke TJ, Kaufmann SH. G(1) and G(2) cell-cycle arrest following microtubule depolymerization in human breast cancer cells. *J Clin Invest* 2002; **110**: 91–99.
41. Masuda A, Maeno K, Nakagawa T, Saito H, Takahashi T. Association between mitotic spindle checkpoint impairment and susceptibility to the induction of apoptosis by anti-microtubule agents in human lung cancers. *Am J Pathol* 2003; **163**: 1109–1116.
42. Bhalla KN Microtubule-targeted anticancer agents and apoptosis. *Oncogene* 2003; **22**: 9075–9086.
43. Castedo M, Perfettini JL,Roumier T, *et al*. Mitotic catastrophe constitutes a special case of apoptosis whose suppression entails aneuploidy. *Oncogene* 2004; **23**: 4362–4370.
44. Casellas P, Galiegue S, Basile AS. Peripheral benzodiazepine receptors and mitochondrial function. *Neurochem Int* 2002; **40**: 475–486.
45. Patterson SD, Spahr CS, Daugas E, *et al.* Mass spectrometric identification of proteins released from mitochondria undergoing permeability transition. *Cell Death Differ* 2000; 7: 137–144.
46. Miccoli L, Poirson-Bichat F, *et al*. Potentiation of lonidamine and diazepam, two agents acting on mitochondria, in human glioblastoma treatment. *J Natl Cancer Inst* 1998; **90**: 1400–1406.
47. Decaudin D, Castedo M, Nemati F, *et al.* Peripheral benzodiazepine receptor ligands reverse apoptosis resistance of cancer cells *in vitro* and *in vivo*. *Cancer Res* 2002; **62**: 1388–1393.
48. Kleinerman RA, Brinton LA, Hoover R, Fraumeni JF Jr. Diazepam use and progression of breast cancer. *Cancer Res* 1984; **44**: 1223–1225.
49. Costantini P, Jacotot E, Decaudin D, Kroemer G. Mitochondrion as a novel target of anticancer chemotherapy. *J Natl Cancer Inst* 2000; **92**: 1042–1053.
50. Guicciardi ME, Leist M, Gores GJ. Lysosomes in cell death. *Oncogene* 2004; **23**: 2881–2890.
51. Cregan SP, Dawson VL, Slack RS. Role of AIF in caspase-dependent and caspase-independent cell death. *Oncogene* 2004; **23**: 2785–2796.
52. Janicke RU, Sprengart ML, Wati MR, Porter AG. Caspase-3 is required for DNA fragmentation and morphological changes associated with apoptosis. *J Biol Chem* 1998; **273**: 9357–9360.
53. Chelli B, Lena A, Vanacore R, *et al.* Peripheral benzodiazepine receptor ligands: Mitochondrial transmembrane potential depolarization and apoptosis induction in rat C6 glioma cells. *Bioch Pharmacol* 2004; **68**: 125–134.